

December 12, 2005
IFJPAN-V-2005-11

Multi-parton Cross Sections at Hadron Colliders

Costas G. Papadopoulos¹ and Małgorzata Worek^{1,2}

¹ *Institute of Nuclear Physics, NCSR Demokritos, 15-310 Athens, Greece*

² *Institute of Nuclear Physics Polish Academy of Sciences
Radzikowskiego 152, 31-3420 Krakow, Poland*

Abstract

We present an alternative method to calculate cross sections for multi-parton scattering processes in the Standard Model at leading order. The helicity amplitudes are computed using recursion relations in the number of particles, which are based on Dyson-Schwinger equations. The summation over colour and helicity configurations are performed by Monte Carlo methods. The computational cost of this algorithm grows asymptotically as 3^n , where n is the number of particles involved in the process, compared to the $n!$ -growth of the more traditional approaches. Results are cross checked with the explicit summation over all colour structures. Typical results for total cross section, differential distributions of the invariant masses, transverse momenta and rapidities of partons are presented. Finally the leading colour approximation and the special helicities approximation have been tested against the exact results.

e-mail: costas.papadopoulos@cern.ch, malgorzata.worek@desy.de

1 Introduction

In high energy collisions among hadrons and leptons, appearing at the operating now TeVatron or in future at the LHC and the e^+e^- Linear Collider, a production of final states with a large number of energetic partons gives rise to events with many jets in the final state. In many cases these multi-jet events offer an important probe of new physics like for example in case of heavy particles decays in the Standard Model and in its extensions like *e.g.* the Minimal Supersymmetric Standard Model. Among them the Higgs boson decay into four jets through W/Z pairs is a well known example. The possibility of identifying new physics relies on precise predictions of the multi-jet rates which usually provide a significant background to those discovery channels as well. The description of these processes is quite difficult because the corresponding amplitudes have to be constructed through a very large number of Feynman diagrams, and thus their automated construction and evaluation becomes the only solution. As an example in the Table 1. the number of Feynman diagrams relevant for calculation of $gg \rightarrow ng$ process are collected. The number of Feynman diagrams grows very fast, asymptotically factorially with the number of particles.

Table 1: *The number of Feynman diagrams contributing to the total amplitude for the $gg \rightarrow ng$ process.*

Process	N_{FG}
$gg \rightarrow 2g$	4
$gg \rightarrow 3g$	25
$gg \rightarrow 4g$	220
$gg \rightarrow 5g$	2485
$gg \rightarrow 6g$	34300
$gg \rightarrow 7g$	559405
$gg \rightarrow 8g$	10525900
$gg \rightarrow 9g$	224449225
$gg \rightarrow 10g$	5348843500

Another aspect of calculating multi-particle amplitudes efficiently is the systematic organisation of the summation over helicity configurations and $SU(N_c)$ colour algebra. If the summation over helicity and colour is performed in a straightforward way then $2^{n_1} \times 3^{n_2}$ helicity configurations and $8^{n_g} \times 3^{n_q} \times 3^{n_{\bar{q}}}$ colour configurations have to be considered, where n_g , n_q , $n_{\bar{q}}$ is the number of gluons, quarks and antiquarks respectively while n_1 stands for the number of fermions and massless bosons and n_2 is the number of the massive vector bosons. Many of these configurations do not give contribution to the amplitude, however, it is very hard to figure out which are in advance. For the processes with many external coloured particles it is necessary to simplify summation over helicity

and colours by the Monte Carlo techniques in order to compute a cross section with sufficient speed to be useful in practise. Apart from handling the number of Feynman diagrams as well as helicity and colour configurations the integration over the multi-dimensional phase space of the final state particles represents a formidable task. In this report we present an approach for the efficient tree level calculation of matrix elements for multi-parton final states which addresses the above problems and therefore improves the currently available techniques [1–4].

The layout of this paper is as follows. In Section 2 the current status on available methods in multi-particle calculations is briefly reviewed. Section 3 describes the colour flow decomposition. We also review two commonly used approximations, which have been proposed for the multi-parton amplitudes. These approximate methods are leading order calculations in colour and the special helicity configurations approximation. Section 4 contains description of the recursive relations and algorithms we used in order to build up the complete amplitude. In section 5 we describe how the calculation in our program is organised. Alternative method for colour structure evaluation is also introduced. The computational complexity of the algorithm is briefly analysed in Section 6. In Section 7 numerical results for the cross sections are presented as well as distributions of the invariant mass, rapidity and transverse momentum are also shown. Moreover, results are compared with already mentioned approximations. The final section contains our summary and an outlook for future improvements of the algorithm. Finally in the Appendix the algorithm for efficient phase space point generation we used in order to obtain our results is described.

2 Dual amplitudes and colour decomposition

For generality we consider the n -gluon scattering

$$g(p_1, \varepsilon_1, a_1) \ g(p_2, \varepsilon_2, a_2) \rightarrow g(p_3, \varepsilon_3, a_3) \dots g(p_n, \varepsilon_n, a_n) \quad (1)$$

with the external momenta $\{p_i\}_1^n$, helicities $\{\varepsilon_i\}_1^n$ and colours $\{a_i\}_1^n$ of gluon $i = 1, \dots, n$. The total amplitude can be expressed as a sum of a single trace terms:

$$\mathcal{M}(\{p_i\}_1^n, \{\varepsilon_i\}_1^n, \{a_i\}_1^n) = 2ig^{n-2} \sum_{P(2, \dots, n)} \text{Tr}(t^{a_1} \dots t^{a_n}) \mathcal{A}(\{p_i\}_1^n, \{\varepsilon_i\}_1^n) \quad (2)$$

where $\alpha_s = g^2/4\pi$ is a gauge coupling and the sum is over $(n-1)!$ permutations of the set $(2, \dots, n)$ and $\text{Tr}(t^{a_1} \dots t^{a_n})$ represents a trace of generators of the $SU(N_c)$ gauge group in the fundamental representation. For processes involving quarks a similar expression can be derived [5]. One of the most interesting aspects of this decomposition is in fact that $\mathcal{A}(\{p_i\}_1^n, \{\varepsilon_i\}_1^n)$ functions, which contain all the kinematic information called dual, partial or colour-ordered amplitudes, are gauge invariant and cyclically symmetric functions of the momenta and helicities of gluons. The colour ordered amplitudes are simpler than the full amplitude because they receive contributions only from diagrams with a particular cyclic ordering of the external gluons (planar graphs). For some processes up to six external partons simple and compact expressions exist in literature [5–11]. Moreover for some special helicity combinations, short analytical forms, called the Parke-Taylor helicity amplitudes or Maximally Helicity violating (MHV) amplitudes, are well known for a general n . They were first obtained by the Parke and Taylor [12] and latter on proved to

be correct through recursive approach by Berends and Giele [13]. The other non vanishing helicity configurations are typically more complicated, however the MHV amplitudes can be used as the basis of approximation schemes for example. Nevertheless, for a large n the scattering processes are still problematic and time consuming. For example to evaluate the full amplitude, the $2^n \times (n-1)!$ configurations of colour ordered amplitudes, have to be considered, where 2^n corresponds to the number of helicity configurations for massless particles. To obtain the cross section from the n -gluon amplitude one has to square and sum over helicity and colour of the external gluons. The squared matrix element can be computed by

$$\sum_{\{a_i\}_1^n \{\varepsilon_i\}_1^n} |\mathcal{M}(\{p_i\}_1^n, \{\varepsilon_i\}_1^n, \{a_i\}_1^n)|^2 = g^{2n-4} \sum_{\varepsilon} \sum_{ij} \mathcal{A}_i \mathcal{C}_{ij} \mathcal{A}_j^* \quad (3)$$

where $(n-1)! \times (n-1)!$ dimensional colour matrix can be written in the most general form as follows:

$$\mathcal{C}_{ij} = \sum_{\{a_i\}_1^n \{\hat{a}_i\}_1^n} \text{Tr}(t^{a_1} \dots t^{a_n}) \text{Tr}(t^{\hat{a}_1} \dots t^{\hat{a}_n})^*. \quad (4)$$

Needless to say that the evaluation of this matrix, is by its own a formidable task in the standard approach.

An important step in the direction of simplification of these calculations has already been obtained by using helicity amplitudes and better organisation of the Feynman diagrams [5, 10, 11, 14–17]. Significant simplification in these calculations has been done by introducing recursive relations [13, 18], which express the n parton currents in terms of all currents up to $(n-1)$ partons. They are based on the smaller building blocks which are just colour ordered vector and spinor currents defined for the off mass shell particles. In the same spirit another approach based on so called ALPHA algorithm [19, 20] or the Dyson-Schwinger recursion equations has been obtained [21–24], where the multi-parton amplitude can be constructed without referring to the individual Feynman diagrams. In the latter case apart from the summation over colour in the colour flow basis, which will be briefly described in the next section, the integration over a continuous set of colour variables (as well as flavour) was introduced. This integration technique, however, does not give a straightforward solution for efficient merging of the parton level calculation with the parton shower evolution.

3 The colour flow decomposition

First let us briefly review the colour approach used in the original version of **HELAC** [22, 23], a multipurpose Monte Carlo generator for multi-particle final states based on the Dyson-Schwinger recursive equations. As was already mentioned, the colour connection or colour flow representation of the interaction vertices was used in this case. This representation has been introduced for the first time in [23] and later on was also studied in [25]. The advantage of this color representation, as compared to the traditional one is that the colour factors acquire a much simpler form, which moreover holds for gluon as well as for quark amplitudes, leading to a unified approach for any tree-order process involving any number of coloured partons. Additionally, the usual information on colour connections, needed by the parton shower Monte Carlo, is automatically available, without any further calculation. In this approach gluon field represented as A_μ^a with $a = 1, \dots, N_c^2 - 1$ is

treated as an $N_c \times N_c$ traceless matrix in colour space [21]. The new object $(A_\mu)_{AB}$ where $A, B = 1, \dots, N_c$ can be obtained by multiplying each gluon field by the corresponding t_{AB}^a matrix as follow:

$$(A_\mu)_{AB} \equiv \sum_{a=1}^{N_c^2-1} t_{AB}^a A_\mu^a. \quad (5)$$

The colour structure of three gluon vertex is given now by, see Fig. 1.:

$$f^{a_1 a_2 a_3} t_{AB}^{a_1} t_{CD}^{a_2} t_{EF}^{a_3} = -\frac{i}{4} (\delta_{AD} \delta_{CF} \delta_{EB} - \delta_{AF} \delta_{CB} \delta_{ED}) \quad (6)$$

where on the right hand side only products of δ 's appear. This colour structure shows how the colour flows in the real physical process, where gluons are represented by colour-anticolour states in the colour space and reflects the fact that colour remain unchanged on an uninterrupted colour line. For a four gluon vertex the following expression has to

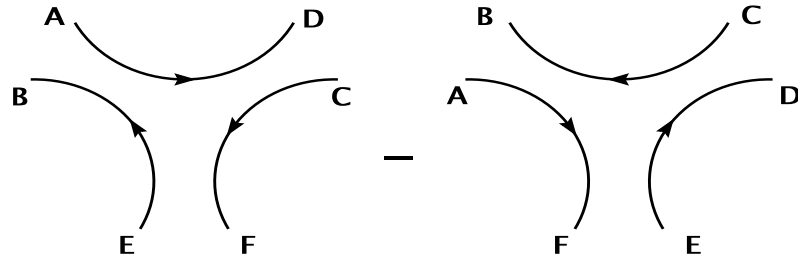


Figure 1: *Colour flows for the three gluon vertex.*

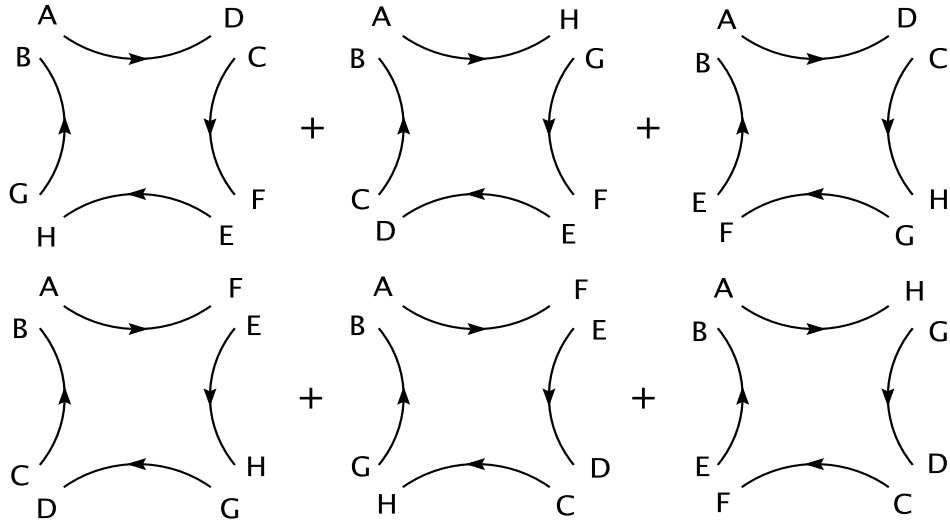


Figure 2: *Colour flows for the four gluon vertex.*

be considered:

$$f^{a_1 a_2 x} f^{x a_3 a_4} t_{AB}^{a_1} t_{CD}^{a_2} t_{EF}^{a_3} t_{GH}^{a_4} \quad (7)$$

with three permutations over $a_1 a_2 a_3$ indices which corresponds to the six colour flows presented in Fig.2. Because gluons can be now in N_c^2 different colour state described for

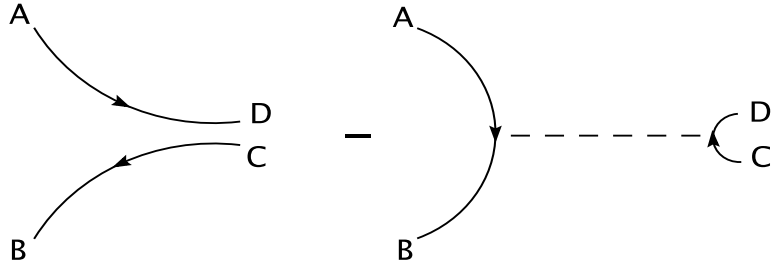


Figure 3: *Colour flows for the $q\bar{q}g$ vertex.*

$N_c = 3$ within the $U(3)$ group we have additional unphysical neutral $U(1)$ gluon. This neutral gluon does not couple to other gluons as can be easily seen from Eq.(6). It couples only to quarks and acts as a colourless particle, see second part of Eq.(8). The colour structure of quark-antiquark-gluon vertex can be described as follows, see Fig.3:

$$t_{AB}^{a_1} t_{CD}^{a_2} = \frac{1}{2} (\delta_{AD} \delta_{CB} - \frac{1}{N_c} \delta_{AB} \delta_{CD}). \quad (8)$$

Let's us introduce more compact notation and associate to each gluon a label (i, σ_i) which refers to the corresponding colour index of previous equations, namely $1 \rightarrow A$, $\sigma_1 \rightarrow B$ and so on. The use of labels will be explained latter on. With this notation the first term of the three gluon vertex is proportional to:

$$\delta_{1\sigma_2} \delta_{2\sigma_3} \delta_{3\sigma_1}. \quad (9)$$

For the same graph with inverted arrows a minus sign and interchanged $i \leftrightarrow j$ has to be included as well. The momentum part of the vertex is still the usual one and in our notation simply given by:

$$g_{12}(p_1 - p_2)^3 + g_{23}(p_2 - p_3)^1 + g_{31}(p_3 - p_1)^2. \quad (10)$$

For the $q\bar{q}g$ vertex we associate a label $(i, 0)$ for quark and $(0, \sigma_i)$ for antiquark. Finally the four gluon vertex is given by a colour factor proportional to:

$$\delta_{1\sigma_3} \delta_{3\sigma_2} \delta_{2\sigma_4} \delta_{4\sigma_1} \quad (11)$$

with six possible permutation, and a Lorentz part

$$2g_{12}g_{34} - g_{13}g_{24} - g_{14}g_{23} \quad (12)$$

where all three permutations should be included.

To make use of the colour representation described so far, let us assign to each external gluon a label $(i, \sigma_I(i))$, to a quark $(i, 0)$ and to antiquark $(0, \sigma_I(i))$, where $i = 1 \dots n$ and $\sigma_I(i), I = 1 \dots n!$ being a permutation of $\{1 \dots n\}$. Since all elementary colour factors appearing in the colour decomposition of the vertices are proportional to δ functions the total colour factor can be given by

$$\mathcal{F}_I = \delta_{1\sigma_I(1)} \delta_{2\sigma_I(2)} \dots \delta_{n\sigma_I(n)}, \quad (13)$$

The colour matrix defined as

$$\mathcal{C}_{IJ} = \sum_{IJ} \mathcal{F}_I \mathcal{F}_J^\dagger \quad (14)$$

with the summation running over all colours, $1, \dots, N_c$ has a very simple representation now

$$\mathcal{C}_{IJ} = N_c^{m(\sigma_I, \sigma_J)} \quad (15)$$

where $1 \leq m(\sigma_I, \sigma_J) \leq n$ counts how many common cycles the permutations σ_I and σ_J have. The practical implementation of these ideas is straightforward. Given the information on the external particles contributing to the process we associate colour labels of the form (i, σ_i) depending on their flavour. According to the Feynman rules the higher level sub-amplitudes are build up. Summing over all $n!$ colour connection configurations, where n is the number of gluons and $q\bar{q}$ pairs in the process using the colour matrix \mathcal{C}_{IJ} we get the total squared amplitude. It is worthwhile to note that summing over all colours configurations is efficient as far as the number of particles is smaller than $\mathcal{O}(6 - 8)$. If the number of gluons and/or $q\bar{q}$ pairs is higher then the number of colour flows, which in general grow like $(n - 1)!$, also start to be problematic from the computational point of view. For multi-colour processes other approaches have to be considered. The natural solution would be to replace the summation over all colours structures by a Monte Carlo over colour configurations. However, Monte Carlo summation is not straightforward in the color flow approach because of the interferences between different colour flows that can give a negative contribution to the squared matrix element.

In the limit $N_c \rightarrow \infty$, only the diagonal terms, $I = J$, survive, and all $\mathcal{O}(N_c^{-2})$ terms can be safely neglected both in the colour matrix and in the $|\mathcal{A}_I|^2$. The interferences between different colour flows vanish in that limit. In the so called Leading Colour Approximation (LCA), the squared amplitude for purely gluonic case is given then by

$$\sum_{a, \varepsilon} |\mathcal{M}(\{p_i\}_1^n, \{\varepsilon_i\}_1^n, \{a_i\}_1^n)|^2 = g^{2n-4} N_c^{n-2} (N_c^2 - 1) \sum_{\varepsilon} \sum_I |\mathcal{A}_I|^2. \quad (16)$$

The term $N_c^2 - 1$ instead of N_c^2 , which of course are equivalent in the limit $N_c \rightarrow \infty$, has been kept in order to reproduce the exact results for $n = 4$ and $n = 5$. In case when $q\bar{q}$ pairs are present the colour factor $N_c^{n-2}(N_c^2 - 1)$ still is the same, however $n = n_g + n_{q\bar{q}}$ in this case, where n_g , $n_{q\bar{q}}$ is the number of gluons and $q\bar{q}$ pairs respectively. This simplification of the colour matrix speed up the calculation moreover, the Monte Carlo summation over colour can be now performed.

Another approximation of the exact calculation is the so called SPecial HELicities approximation (SPHEL). It is based on the fact that for certain helicity configurations of the partons, the MHV amplitudes, short analytical expressions exist. The special helicity configurations are the ones where all but two partons have the same helicity when all the momenta are outgoing. In the purely gluonic case when all gluons or all but one have the same helicity the corresponding amplitudes vanishes. The special helicity configurations are simply the first configurations for which $\mathcal{A} \neq 0$. Here the assumption is made that those special configurations are typical for all possible configurations in the process under consideration. Since the dominant processes are always given by the purely gluonic ones and by increasing the number of $q\bar{q}$ pairs the contributions coming from those subprocesses become less and less important it seems to be a good approximation¹. The

¹Although as it has been shown in [24], the percentage of the pure gluonic contribution decreases as a function of the number of the external legs

second assumption of SPHEL is that the non-leading colour contributions are neglected as in the LCA approach. The precise expression for SPHEL depends on number of quarks present [17, 18] and for purely gluonic case is given by:

$$\sum_{a,\varepsilon} |\mathcal{M}(\{p_i\}_1^n, \{\varepsilon_i\}_1^n, \{a_i\}_1^n)|^2 = 2g^{2n-4} N_c^{n-2} (N_c^2 - 1) \times \quad (17)$$

$$\frac{2^n - 2(n+1)}{n(n-1)} \sum_{1 \leq i \leq j \leq n} (p_i \cdot p_j)^4 \sum_{P(2, \dots, n)} \frac{1}{(p_1 \cdot p_2)(p_2 \cdot p_3) \dots (p_n \cdot p_1)},$$

where the sum runs over all permutations of the set $(2, \dots, n)$. The factor $n(n-1)$ counts the number of MHV amplitudes for the n gluon process. The total number of non zero helicity amplitudes is instead $2^n - 2(n+1)$. For $n = 4$ there is a double counting and the result should be corrected by the factor $1/2$. For $n = 4, 5$ this formula describes exact results as it well known. There are no known expressions for special helicity configurations with more than two massless quark pairs so SPHEL does not work for processes with more than 2 $q\bar{q}$ pairs.

4 Dyson-Schwinger recursion relations

Let us present now the recursive relations based on Dyson-Schwinger equations for the calculation of the partial amplitudes. These equations give recursively the n -point Green's functions in terms of the $1-$, $2-$, \dots , $(n-1)-$ point functions. They hold all the information for the fields and their interactions for any number of external legs and to all orders in perturbation theory. We will concentrate here on the gluon, quark and anti-quark recursion relations, however, in the same way recursive equations for leptons and gauge bosons can be obtained. The diagrammatic picture behind the recursive relation is actually quite simple. The tree-order recursive equation can be diagrammatically presented as is shown in Fig.4. Let p_1, p_2, \dots, p_n represent the external momenta involved in the scattering process taken to be incoming. In order to write down the recursive relation explicitly first we define a set of four vectors $[A^\mu(P); (A, B)]$, which describes any sub-amplitudes from which a gluon with momentum P and colour-anticolour assignment A, B can be constructed. The momentum P is given as a sum of external particles momenta. Accordingly we define a set of four-dimensional spinors $[\psi(P); (A, 0)]$ describing any sub-amplitude from which a quark with momentum P and colour A can be constructed and by $[\bar{\psi}(P); (0, B)]$ a set of four-dimensional antispinors for antiquark with anticolour B . The

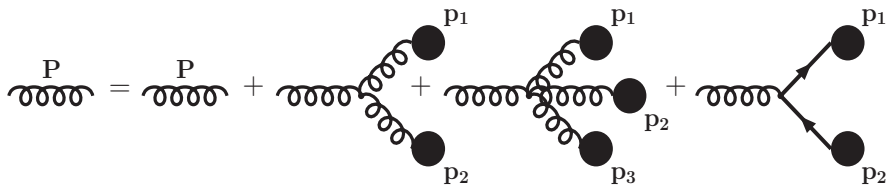


Figure 4: *Recursive equation for an off mass shell gluon of momentum P .*

Dyson-Schwinger recursion equation for gluon in a general way can be written as follows:

$$[A^\mu(P); (A, B)] = \sum_{i=1}^n [\delta(P - p_i) A^\mu(p_i); (A, B)_i] \quad (18)$$

$$\begin{aligned}
& + \sum_{P=p_1+p_2} [(ig) \Pi_\rho^\mu V^{\rho\nu\lambda}(P, p_1, p_2) A_\nu(p_1) A_\lambda(p_2) \sigma(p_1, p_2); (A, B) = (C, D)_1 \otimes (E, F)_2] \\
& - \sum_{P=p_1+p_2+p_3} [(g^2) \Pi_\sigma^\mu G^{\sigma\nu\lambda\rho}(P, p_1, p_2, p_3) A_\nu(p_1) A_\lambda(p_2) A_\rho(p_3) \sigma(p_1, p_2 + p_3); \\
& \quad (A, B) = (C, D)_1 \otimes (E, F)_2 \otimes (G, H)_3] \\
& + \sum_{P=p_1+p_2} [(ig) \Pi_\nu^\mu \bar{\psi}(p_1) \gamma^\nu \psi(p_2) \sigma(p_1, p_2); (A, B) = (0, D)_1 \otimes (C, 0)_2]
\end{aligned}$$

where $A, B, C, D, E, F, G, H = 1, 2, 3$. The rules for merging colour and anticolour of the particles which are combined will be explained in the next section. The $V^{\mu\nu\lambda}(P, p_1, p_2)$ and $G^{\mu\nu\lambda\rho}(P, p_1, p_2, p_3)$ functions are the three- and four-gluon vertices presented in the previous sections and the symbol $\sigma(p_1, p_2)$ is the sign function which takes into account the Fermi sign when two identical fermions are interchanged and has the values ± 1 . The exact form of this function can be found in Ref. [22, 24]. The sums are over all combinations of p_1, p_2 or p_1, p_2, p_3 that sum up to P . The propagator for gluon is given by:

$$\Pi_{\mu\nu} = \frac{-ig_{\mu\nu}}{P^2}. \quad (19)$$

For a quark of momentum P we have, Fig.5:

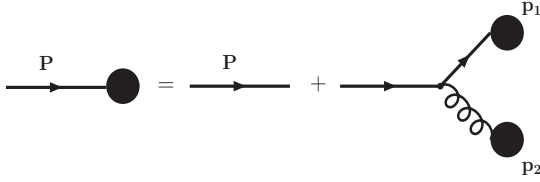


Figure 5: Recursive equation for an off mass shell quark of momentum P .

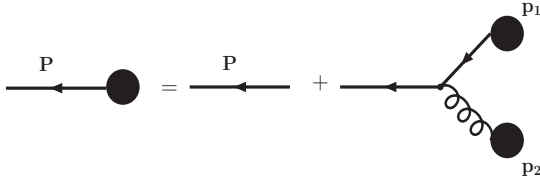


Figure 6: Recursive equation for an off mass shell antiquark of momentum P .

$$[\psi(P); (A, 0)] = \sum_{i=1}^n [\delta(P - p_i) \psi(p_i); (A, 0)_i] \quad (20)$$

$$+ \sum_{P=p_1+p_2} [(ig) \mathcal{P} A^\mu(p_1) \gamma_\mu \psi(p_2) \sigma(p_1, p_2); (A, 0) = (B, C)_1 \otimes (D, 0)_2]$$

where \mathcal{P} is the propagator

$$\mathcal{P} = \frac{iP}{P^2}. \quad (21)$$

Finally for an antiquark, Fig.6:

$$[\bar{\psi}(P); (0, A)] = \sum_{i=1}^n [\delta(P - p_i) \bar{\psi}(p_i); (0, A)_i] \quad (22)$$

$$+ \sum_{P=p_1+p_2} [(ig) \bar{\psi}(p_2) A^\mu(p_1) \gamma_\mu \bar{\mathcal{P}} \sigma(p_1, p_2); (0, A) = (B, C)_1 \otimes (0, D)_2]$$

where

$$\bar{\mathcal{P}} = \frac{-iP}{P^2}. \quad (23)$$

In the same spirit the recursion equations for all leptons and gauge bosons can be written down. With this algorithm we can thus compute the scattering amplitude for any initial and final states taking into account particles masses as well. In particular any colour structure can be assigned to the external legs. Finally this approach has an exponential growth of computational time with the number of external particles instead of factorial growth in case when traditional Feynman graphs are considered. It can be farther optimised in order to reduce computational complexity by replacing each four gluon vertex by a three particle vertex by introducing the auxiliary field represented by the antisymmetric tensor $H_{\mu\nu}^a$. This new field has quadratic term without derivatives so has no independent dynamics. The part of the QCD Lagrangian that describes the four gluon vertex

$$\mathcal{L} = -\frac{1}{4} F_{\mu\nu}^a F^{\mu\nu a}, \quad F_{\mu\nu}^a = \partial_\mu A_\nu^a - \partial_\nu A_\mu^a + g f^{abc} A_\mu^b A_\nu^c \quad (24)$$

can be rewrite in term of the auxiliary field as follows:

$$\mathcal{L} = -\frac{1}{2} H_{\mu\nu}^a H^{\mu\nu a} + \frac{1}{4} H_{\mu\nu}^a F^{\mu\nu a}. \quad (25)$$

A single interaction term of the form $H^{\mu\nu a} A_\mu^b A_\nu^c$ is left only, instead of interaction terms represented by Eq.(24). Diagrammatically, the elimination of the four gluon vertex can be understood as in Fig.7. The recursion for the gluons now changes slightly, in fact only

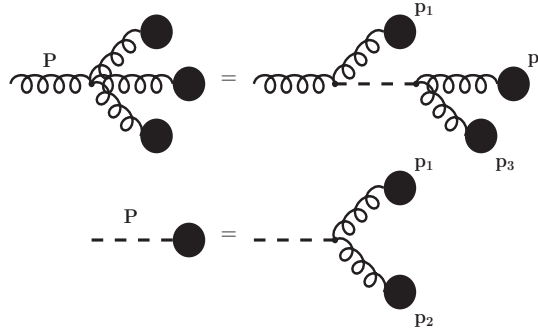


Figure 7: *Elimination of the four-gluon vertex by the auxiliary field and new recursive equation for an auxiliary field of momentum P .*

for the four-gluon vertex part, however, we have an additional equation for the auxiliary field:

$$[A^\mu(P); (A, B)] = \sum_{i=1}^n [\delta(P - p_i) A^\mu(p_i); (A, B)_i] \quad (26)$$

$$\begin{aligned}
& + \sum_{P=p_1+p_2} [(ig) \Pi_\rho^\mu V^{\rho\nu\lambda}(P, p_1, p_2) A_\nu(p_1) A_\lambda(p_2) \sigma(p_1, p_2); (A, B) = (C, D)_1 \otimes (E, F)_2] \\
& + \sum_{P=p_1+p_2} [(ig) \Pi_\sigma^\mu (g^{\sigma\lambda} g^{\nu\rho} - g^{\nu\lambda} g^{\sigma\rho}) A_\nu(p_1) H_{\lambda\rho}(p_2) \sigma(p_1, p_2); (A, B) = (C, D)_1 \otimes (E, F)_2] \\
& \quad + \sum_{P=p_1+p_2} [(ig) \Pi_\nu^\mu \bar{\psi}(p_1) \gamma^\nu \psi(p_2) \sigma(p_1, p_2); (A, B) = (0, D)_1 \otimes (C, 0)_2]
\end{aligned}$$

and

$$\begin{aligned}
[H^{\mu\nu}(P); (A, B)] &= \sum_{P=p_1+p_2} [(ig) (g^{\mu\lambda} g^{\nu\rho} - g^{\nu\lambda} g^{\mu\rho}) A_\lambda(p_1) A_\rho(p_2) \sigma(p_1, p_2); (A, B) = (C, D)_1 \otimes (E, F)_2] \\
(A, B) &= (C, D)_1 \otimes (E, F)_2.
\end{aligned} \tag{27}$$

Few comments are in order now. First, all calculations were performed in the light cone representation and all momenta are taken to be incoming. Second, this new $H_{\mu\nu}$ field has six components. Additionally as we can see in Eq.(26) and Eq.(27) the colour structure of this new vertices, remain the same as in case of the three gluon vertex. The number of the types of the sub-amplitudes one has to calculate now is in general doubled, however their structure is much simpler, which save computational time while the iteration steps are performed.

After $n - 1$ steps, where n is the number of particles under consideration, one can get the total amplitude. The scattering amplitude can be calculated by any of the following relations, depending on the process under consideration,

$$\mathcal{A}(\{p_i\}_1^n, \{\varepsilon_i\}_1^n) = \begin{cases} \hat{A}^\mu(P_i) A_\mu(p_i) & \text{where } i \text{ corresponds to gluon} \\ \hat{\bar{\psi}}(P_i) \psi(p_i) & \text{where } i \text{ corresponds to quark line} \\ \bar{\psi}(p_i) \hat{\psi}(P_i) & \text{where } i \text{ corresponds to antiquark line} \end{cases} \tag{28}$$

where

$$P_i = \sum_{j \neq i} p_j,$$

so that $P_i + p_i = 0$. The functions with hat are given by the previous expressions except for the propagator term which is removed by the amputation procedure. This is because the outgoing momentum P_i must be on shell. The initial conditions are given by

$$\begin{aligned}
A^\mu(p_i) &= \epsilon_\lambda^\mu(p_i), \lambda = \pm 1, 0 \\
\psi(p_i) &= \begin{cases} u_\lambda(p_i) & \text{if } p_i^0 \geq 0 \\ v_\lambda(-p_i) & \text{if } p_i^0 \leq 0 \end{cases} \\
\bar{\psi}(p_i) &= \begin{cases} \bar{u}_\lambda(p_i) & \text{if } p_i^0 \geq 0 \\ \bar{v}_\lambda(-p_i) & \text{if } p_i^0 \leq 0 \end{cases}
\end{aligned} \tag{29}$$

where the explicit form of $\epsilon_\lambda^\mu, u_\lambda, v_\lambda, \bar{u}_\lambda, \bar{v}_\lambda$ are given in the Ref. [22].

In order to actually solve these recursive equations it is convenient to use a binary representation of the momenta involved [19]. For a process with n external particles, to the momentum P^μ defined as

$$P^\mu = \sum_{i=1}^n p_i^\mu \tag{30}$$

a binary vector $\vec{m} = (m_1, \dots, m_n)$ can be assigned, where its components take the values 0 or 1, in such a way that

$$P^\mu = \sum_{i=1}^n m_i p_i^\mu. \quad (31)$$

Moreover this binary vector can be uniquely represented by the integer

$$m = \sum_{i=1}^n 2^{i-1} m_i \quad (32)$$

where

$$1 \leq m \leq 2^n - 1. \quad (33)$$

Therefore all sub-amplitudes can be labeled accordingly, *i.e.*

$$\begin{aligned} \psi(P) &\rightarrow \psi(m), \\ \bar{\psi}(P) &\rightarrow \bar{\psi}(m), \\ A^\mu(P) &\rightarrow A^\mu(m). \end{aligned} \quad (34)$$

If the particle number 1 is chosen as the ending point in the calculation then all sub-amplitudes where the momentum p_1 does not appear are only evaluated. This excludes all odd integers between 1 and $2^n - 2$. A very convenient ordering of integers in binary representation relies on the notion of level l , defined simply as

$$l = \sum_{i=1}^n m_i. \quad (35)$$

As it is easily seen all external momenta are of level 1, whereas the total amplitude corresponds to the unique level n integer $2^n - 1$. This ordering dictates the natural path of the computation; starting with level-1 sub-amplitudes, we compute the level-2 ones using the Dyson-Schwinger equations and so on up to the level n which is the full amplitude.

5 Organisation of the calculation

The recursive algorithm presented in the previous section has the advantage that any colour representation can be used in order to assign colour degrees of freedom to the external legs in the process under consideration. It can be used either for colour ordered amplitudes or for the full amplitude as well. The latter case is in fact the topic of this section. Moreover, an alternative method for taking into account the colour structure of scattering partons, based on regular colour configuration assignments as compared to colour flow ones, will be introduced. First, however, the organisation of the calculation will be shortly explained in order to better understand the general structure. Contrary to the original **HELAC** [22, 23] approach, in this new version the computational part consists of one phase only. This is not optimal for electroweak processes with moderate number of external particles, but it becomes quite efficient for processes with many particles, especially when only a few species of particles are involved (scalar amplitudes, gluon amplitudes in QCD, etc). The vertices described by the Standard Model Lagrangian

are implemented in fusion rules that dictate the way the subamplitudes, at each level of the recursion relation, will be merged, in order to produce a higher level subamplitude. In case when quark with antiquark is combined, for example, there are three possible subamplitudes which describe three different intermediate states incorporated inside the fusion rules, namely γ , Z and g .

Let us present now the colour merging rules which are evaluated iteratively at the subamplitude level as well. During each iteration when two particles are combined their corresponding colour assignments are combined as well. To obtain a gluon (A, B) described by recursive relation Eq.(26) we have three possibilities. First, it can be obtained when quark with colour assignment $(C, 0)$ is merged with the antiquark of anticolour $(0, D)$. Second, when two gluons (C, D) and (E, F) are combined, where $A, B, C, D, E, F = 1, \dots, 3$. And finally when a gluon and an auxiliary field H are combined: in this case, the colour structure of the vertex is identical to the three-gluon vertex. So we end up with the following rules:

$$(A, B) = (C, 0) \otimes (0, D), \quad (36)$$

$$(A, B) = (C, D) \otimes (E, F). \quad (37)$$

In the first case the merging is occurring according to the rule presented in Eq.(8). and the following gluon can be produced:

$$(A, B) = (C, 0) \otimes (0, D) = (C, D), \quad \text{if } C \neq D. \quad (38)$$

Let's us present a simple example. For a quark with $(1, 0)$ colour and for antiquark with $(0, 3)$ anticolour we have one possibility mainly $(1, 0) \otimes (0, 3) \rightarrow (1, 3)$ state with weight 1. The factor $1/2$ in front of the Eq.(8) is taken into account in the coupling constant normalisation. However, the situation is more complex when quark and antiquark have the same colour and anticolour:

$$(A, B) = (C, 0) \otimes (0, D) = (1, 1) \oplus (2, 2) \oplus (3, 3), \quad \text{if } C = D. \quad (39)$$

We have three possibilities with different weights. Again in a simple example, for $(1, 0)$ and $(0, 1)$ we have $(1, 1) \oplus (2, 2) \oplus (3, 3)$ with corresponding weight $2/3$, $-1/3$ and $-1/3$.

In the second case, when gluons are combined according to Eq.(6) we have the following options:

$$(A, B) = (C, D) \otimes (E, F) = (E, D), \quad \text{if } C = F \quad (40)$$

$$(A, B) = (C, D) \otimes (E, F) = (C, F), \quad \text{if } D = E. \quad (41)$$

So for example when $(1, 2)$ and $(2, 3)$ gluons are combined the $(1, 2) \otimes (2, 3) \rightarrow (1, 3)$ gluons is gained with weight -1 . Again the factor in front of the Eq.(6) was included in the overall normalisation. Moreover, we have additional possibility when colours and anticolours of gluons are the same, then for example for $(1, 2)$ and $(2, 1)$ case one gets gluon into two colour states namely $(1, 1)$ and $(2, 2)$ with different weight, $-1, 1$ respectively.

To obtain the quark, $(A, 0)$, described by the recursive relation Eq.(20) we have to combine gluon with another quark one more time according to the rule presented in Eq.(8):

$$(A, 0) = (B, C) \otimes (D, 0). \quad (42)$$

We have two possibilities for colour assignment:

$$(A, 0) = (B, C) \otimes (D, 0) = (B, 0), \quad \text{if } C = D, \quad (43)$$

$$(A, 0) = (B, C) \otimes (D, 0) = (D, 0), \quad \text{if } B = C. \quad (44)$$

As an example consider $(1, 2)$ gluons and $(2, 0)$ quark, as the result one can obtain quark $(1, 2) \otimes (2, 0) \rightarrow (1, 0)$ with weight $-1/3$. When colour and anticolour of gluon are the same we have the following situation $(2, 2) \otimes (3, 0) \rightarrow (3, 0)$ with the weight 1. Moreover when quark has the same color as gluon the new quark again remain in its colour state $(2, 2) \otimes (2, 0) \rightarrow (2, 0)$ but with the different weight $2/3$. For the antiquark the situation is the same, so we will not elaborate it here.

For the $q\bar{q}$ interactions with γ, Z^0, W^\pm or Higgs boson the situation is very simple and we have only one possibility:

$$(A, 0) \otimes (0, B) = (0, 0) \quad \text{if } A = B. \quad (45)$$

The sum over colour can be performed in this way by considering all possible colour-anticolour configurations according to those rules. However, the procedure can be facilitated by Monte Carlo methods where the particular colour-anticolour configuration is randomly selected. Then the corresponding contribution to the amplitude squared is evaluated. Assuming that, on average, all colour configurations contribute the same amount to the cross section this approach is numerically more efficient than summing each event over all colours. The *necessary* condition which must be fulfilled, while the particular colour assignment for the external coloured particles is chosen, is that the number of colour and anticolour of each type, is the same. Otherwise the particles can not be connected by colour flow lines and the amplitude is identically zero. In the Monte Carlo over colour method one has to multiply the squared matrix element by a coefficient that counts the number of non zero colour configurations.

The number of non zero colour configurations, according to the above mentioned necessary condition is given by

$$N_{CC} = \sum_{A=0}^{n_q} \sum_{B=0}^{n_q-1} \sum_{C=0}^{n_q-A-B} \left(\frac{n_q!}{A!B!C!} \right)^2 \delta(n_q = A + B + C) \quad (46)$$

where n_q is the total number of quarks and A, B, C are the numbers of quarks of the colour type 1, 2 and 3 respectively. The weight of the event for which a non-vanishing colour configuration was chosen randomly is proportional to $|M|^2$ multiplied by N_{CC} . As we already stated, the condition given by Eq.(46) is necessary but not sufficient. Among this set there are still configurations which do not give contributions to the total amplitude.

In Tab. 2. and Tab. 3. different numbers of colour configurations in the process under consideration are presented. In the first column of the Tab. 2. and Tab. 3 the total number of all colour configurations are listed, where $N_{CC}^{\text{ALL}} = 3^{n_q+n_{\bar{q}}}$ and $n_q, n_{\bar{q}}$ are the number of quarks and antiquarks respectively and gluons are treated as $q\bar{q}$ pairs. The second column represent the results for the number of non vanishing colour configurations N_{CC} calculated using formula Eq.(46). The number of colour configurations (in percentage) inside the N_{CC} set which finally give rise to non zero amplitudes are shown in the last column of Tab. 2. and Tab. 3. Those numbers N_{CC}^F are evaluated by the Monte Carlo. Note that while the number of external particles is increased the corresponding number of vanishing colour configurations in the third column is decreased, as we can see in Tab. 2.

Table 2: *The number of colour configurations for the processes with gluons only. N_{CC}^{ALL} corresponds to all possible colour configurations, while N_{CC} corresponds to the number of colour configurations calculated using formula Eq.(46). In the last column the number of non vanishing colour configurations evaluated by MC N_{CC}^{F} (in percentage) inside the N_{CC} is shown.*

Process	N_{CC}^{ALL}	N_{CC}	$N_{CC}^{\text{F}} (\%)$
$gg \rightarrow 2g$	6561	639	59.1
$gg \rightarrow 3g$	59049	4653	68.4
$gg \rightarrow 4g$	531441	35169	77.4
$gg \rightarrow 5g$	4782969	272835	85.0
$gg \rightarrow 6g$	43046721	2157759	90.4
$gg \rightarrow 7g$	387420489	17319837	94.0
$gg \rightarrow 8g$	3486784401	140668065	96.4

As far as the summation over the helicity configurations is concerned there are two possibilities, either the explicit summation over all helicity configurations or a Monte Carlo approach. In the latter case, for example for gluon, it is achieved by introducing the polarisation vector

$$\varepsilon_\phi^\mu(p) = e^{i\phi} \varepsilon_+^\mu(p) + e^{-i\phi} \varepsilon_-^\mu(p), \quad (47)$$

where $\phi \in (0, 2\pi)$. By integrating over ϕ we can obtain the sum over helicities

$$\frac{1}{2\pi} \int_0^{2\pi} d\phi \, \varepsilon_\phi^\mu(p) (\varepsilon_\phi^\nu(p))^* = \sum_{\lambda=\pm} \varepsilon_\lambda^\mu(p) (\varepsilon_\lambda^\nu(p))^*.$$

6 Computational cost of the algorithm

To determine the cost for computation of the n -point amplitude using the algorithm based on Dyson-Schwinger equations, one has to counts how many operation should be done [26]. There are $\binom{n}{k}$ momenta at each level. The total amount of sub-amplitudes corresponding to those momenta is simply given by:

$$\sum_{k=1}^{n-1} \binom{n}{k} = 2^n - 2 \quad (48)$$

where n is the number of particles involving in the calculation. Moreover one has to count how many way exist to split a number of level k to two numbers of levels k_1 and k_2 . The last step is to sum over all levels. The total number of operation should be performed in

Table 3: *The number of colour configurations for the processes with gluons and one or two $q\bar{q}$ pairs. N_{CC}^{ALL} corresponds to all possible colour configurations, while N_{CC} corresponds to the number of colour configurations calculated using formula Eq.(46). In the last column the number of non vanishing colour configurations evaluated by MC N_{CC}^F (in percentage) inside the N_{CC} is shown.*

Process	N_{CC}^{ALL}	N_{CC}	N_{CC}^F (%)
$gg \rightarrow u\bar{u}$	729	93	93.5
$gg \rightarrow g u\bar{u}$	6561	639	91.6
$gg \rightarrow 2g u\bar{u}$	59049	4653	92.6
$gg \rightarrow 3g u\bar{u}$	531441	35169	94.6
$gg \rightarrow 4g u\bar{u}$	4782969	272835	96.4
$gg \rightarrow 5g u\bar{u}$	43046721	2157759	97.8
$gg \rightarrow 6g u\bar{u}$	387420489	17319837	98.6
<hr/>			
$gg \rightarrow c\bar{c}c\bar{c}$	6561	639	99.1
$gg \rightarrow g c\bar{c}c\bar{c}$	59049	4653	98.8
$gg \rightarrow 2g c\bar{c}c\bar{c}$	531441	35169	99.0
$gg \rightarrow 3g c\bar{c}c\bar{c}$	4782969	272835	99.3
$gg \rightarrow 4g c\bar{c}c\bar{c}$	43046721	2157759	99.6

case when only three-point vertices exist is then

$$\sum_{k=1}^{n-1} \binom{n}{k} \sum_{l=1}^{k-1} \binom{k}{l} = \sum_{k=1}^{n-1} \binom{n}{k} \{2^k - 2\} = 3^n - 3 \cdot 2^n + 3. \quad (49)$$

In the limit $n \rightarrow \infty$ the number of operations grow like 3^n instead of the $n!$ growth in the traditional Feynman graph approach. When the Monte Carlo over colour structures is performed and only one particular colour configuration is randomly chosen the computational cost of this algorithm is given exactly by this expression. Otherwise, this formula must be multiply by the number of non zero colour configurations for the process under consideration.

7 Numerical Results

In this section numerical results on multi-parton production at LHC are presented. In particular we are interested in two subjects. First, to which extend the Monte Carlo summation over colour, which enormously speed up the calculation, can give results with comparable precision as the one based on an explicit summation, and second, whether

several approximations, like the LCA and the SPHEL, can reliably describe the physical process.

The centre of mass system energy was chosen to be $\sqrt{s} = 14$ TeV. In order to stay in the perturbative safe region and to simulate as much as possible experimentally relevant phase-space regions, we have chosen the following cuts:

$$p_{T_i} > 60 \text{ GeV}, \quad |y_i| < 2.5, \quad \Delta R_{ij} > 1.0 \quad (50)$$

for each pair of outgoing partons i and j . Here p_{T_i} and y_i are the transverse momentum and rapidity of a parton respectively defined as:

$$p_{T_i} = \sqrt{p_{x_i}^2 + p_{y_i}^2}, \quad y_i = \frac{1}{2} \ln \left(\frac{E_i + p_{z_i}}{E_i - p_{z_i}} \right). \quad (51)$$

In practice for massless quarks the rapidity is often replaced by the pseudorapidity variable $\eta = -\ln \tan(\theta/2)$, where θ is an angle from the beam direction measured directly in the detector. The last variable is ΔR_{ij} which is a radius of cone of the parton defined as

$$\Delta R_{ij} = \sqrt{(\Phi_i - \Phi_j)^2 + (\eta_i - \eta_j)^2} \quad (52)$$

with azimuthal angle $\Delta\Phi_{ij} = \Phi_i - \Phi_j \in (0, \pi)$

$$\Delta\Phi_{ij} = \arccos \left(\frac{p_{x_i}p_{x_j} + p_{y_i}p_{y_j}}{p_{T_i}p_{T_j}} \right). \quad (53)$$

Quarks are treated as massless. All results are obtained with a fixed strong coupling constant ($\alpha_s=0.13$). For the parton structure functions, we used CTEQ6 PDF's parametrisation [27, 28]. For the phase space generation we used the algorithm described in the Appendix, whereas in several cases results were cross checked with

- PHEGAS [29], which construct automatically mappings of all possible peaking structures of a given scattering process and uses self-adaptive procedures like multi-channel optimisation [30],
- HAAG [31], which efficiently map the so called “antenna momentum structures” typically occurring in the QCD amplitudes, and
- RAMBO [32], a flat phase-space generator.

Total rates and various kinematical distributions are examined. The algorithm described in the previous sections as well as in Ref. [33, 34] has been used to compute total cross sections for many parton production. We give the result with summation over all possible colour configurations, called 'exact', σ_{EXACT} , as well as the result obtained with Monte Carlo summation over colour σ_{MC} .

In case of the explicit summation both colour flow and colour configuration decomposition has been used to cross check results. Additionally two approximations are tested namely LCA and SPHEL. As far as helicity summation is concerned, a Monte Carlo over helicity is applied.

The results presented for the total cross sections, have been obtained for 10^6 Monte Carlo points passing the selection cuts given by Eq.(50). In the Tab. 4. the results for

Table 4: *Results for the total cross section for processes with gluons and quarks with up to two $q\bar{q}$ pairs. σ_{EXACT} corresponds to summation over all possible colour configurations, while σ_{MC} corresponds to Monte Carlo summation.*

Process	$\sigma_{\text{EXACT}} \pm \varepsilon$ (nb)	ε (%)	$\sigma_{\text{MC}} \pm \varepsilon$ (nb)	ε (%)
$gg \rightarrow 2g$	$(0.46572 \pm 0.00258) \times 10^4$	0.5	$(0.46849 \pm 0.00308) \times 10^4$	0.6
$gg \rightarrow 3g$	$(0.15040 \pm 0.00159) \times 10^3$	1.0	$(0.15127 \pm 0.00110) \times 10^3$	0.7
$gg \rightarrow 4g$	$(0.11873 \pm 0.00224) \times 10^2$	1.9	$(0.12116 \pm 0.00134) \times 10^2$	1.1
$gg \rightarrow 5g$	$(0.10082 \pm 0.00198) \times 10^1$	1.9	$(0.09719 \pm 0.00142) \times 10^1$	1.5
$gg \rightarrow 6g$	$(0.74717 \pm 0.01490) \times 10^{-1}$	2.0	$(0.76652 \pm 0.01862) \times 10^{-1}$	2.4
$gg \rightarrow u\bar{u}$	$(0.36435 \pm 0.00199) \times 10^2$	0.5	$(0.36619 \pm 0.00132) \times 10^2$	0.4
$gg \rightarrow g\bar{u}$	$(0.35768 \pm 0.00459) \times 10^1$	1.3	$(0.35466 \pm 0.00291) \times 10^1$	0.8
$gg \rightarrow 2g\bar{u}$	$(0.49721 \pm 0.00758) \times 10^0$	1.5	$(0.50053 \pm 0.00725) \times 10^0$	1.4
$gg \rightarrow 3g\bar{u}$	$(0.50598 \pm 0.01441) \times 10^{-1}$	2.8	$(0.52908 \pm 0.01264) \times 10^{-1}$	2.4
$gg \rightarrow 4g\bar{u}$	$(0.51549 \pm 0.02017) \times 10^{-2}$	3.9	$(0.51581 \pm 0.01245) \times 10^{-2}$	2.4
$gg \rightarrow c\bar{c}c\bar{c}$	$(0.25190 \pm 0.00528) \times 10^{-2}$	2.1	$(0.24903 \pm 0.00373) \times 10^{-2}$	1.5
$gg \rightarrow g\bar{c}c\bar{c}$	$(0.60196 \pm 0.01908) \times 10^{-3}$	3.2	$(0.58817 \pm 0.00926) \times 10^{-3}$	1.6
$gg \rightarrow 2g\bar{c}c\bar{c}$	$(0.95682 \pm 0.03441) \times 10^{-4}$	3.6	$(0.92212 \pm 0.02485) \times 10^{-4}$	2.7

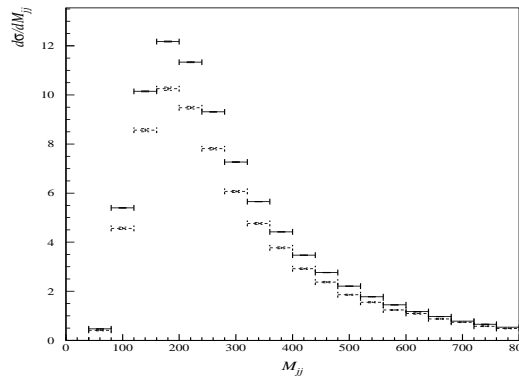


Figure 8: *Invariant mass distribution of 2 gluons in the $gg \rightarrow 4g$ process. Solid line crosses denote SPHEL case whereas dashed, the Monte Carlo one.*

the total cross section for processes with gluons and quarks with up to two $q\bar{q}$ pairs are presented. We compare in this table result for the summation over all possible colour

Table 5: *Results for the total cross section for processes with gluons, Z , W^\pm and quarks with up to $q\bar{q}$ pairs for the higher number of external partons. σ_{MC} corresponds to Monte Carlo summation over colour.*

Process	$\sigma_{\text{MC}} \pm \varepsilon$ (nb)	ε (%)
$gg \rightarrow 7g$	$(0.53185 \pm 0.01149) \times 10^{-2}$	2.1
$gg \rightarrow 8g$	$(0.33330 \pm 0.00804) \times 10^{-3}$	2.4
$gg \rightarrow 9g$	$(0.17325 \pm 0.00838) \times 10^{-4}$	4.8
$gg \rightarrow 5gu\bar{u}$	$(0.38044 \pm 0.01096) \times 10^{-3}$	2.8
$gg \rightarrow 3gc\bar{c}c\bar{c}$	$(0.95109 \pm 0.02456) \times 10^{-5}$	2.6
$gg \rightarrow 4gc\bar{c}c\bar{c}$	$(0.81400 \pm 0.02583) \times 10^{-6}$	3.2
$gg \rightarrow Zu\bar{u}gg$	$(0.18948 \pm 0.00344) \times 10^{-3}$	1.8
$gg \rightarrow W^+\bar{u}dgg$	$(0.62704 \pm 0.01458) \times 10^{-3}$	2.3
$gg \rightarrow ZZu\bar{u}gg$	$(0.16217 \pm 0.00420) \times 10^{-6}$	2.6
$gg \rightarrow W^+W^-u\bar{u}gg$	$(0.27526 \pm 0.00752) \times 10^{-5}$	2.7
$d\bar{d} \rightarrow Zu\bar{u}gg$	$(0.38811 \pm 0.00569) \times 10^{-5}$	1.5
$d\bar{d} \rightarrow W^+\bar{c}sgg$	$(0.18765 \pm 0.00453) \times 10^{-5}$	2.4
$d\bar{d} \rightarrow ZZgggg$	$(0.99763 \pm 0.02976) \times 10^{-7}$	2.9
$d\bar{d} \rightarrow W^+W^-gggg$	$(0.52355 \pm 0.01509) \times 10^{-6}$	2.9

configurations, σ_{EXACT} with the results where the explicit summation is replaced by the Monte Carlo one, σ_{MC} . All cross sections are in agreement within the error. For the same number of accepted events the results with the Monte Carlo summation over colour can be obtained much faster and the error is at the same level or even smaller compared to the 'exact' results for the same processes.

In the next Tab. 5. the results for the total cross section for processes with gluon, Z , W^\pm and quarks with up to $q\bar{q}$ pairs for a larger number of external partons are also presented.

Results for the total cross section in the leading colour approximation (LCA), σ_{LCA} , are listed in Tab. 6. The LCA is exact for $n = 4$, and $n = 5$ for purely gluonic case. Finally results in the special helicities approximation (SPHEL) for the total cross section σ_{SPHEL} , are shown in Tab. 7. For the $gg \rightarrow 2g$ and $gg \rightarrow 3g$ processes SPHEL gives exact result for the total cross section as we can see in the Tab. 7. SPHEL approximation gives results for the total cross section greater than those of the exact for $gg \rightarrow ng$ processes,

Table 6: *Results for the total cross section in the leading colour approximation (LCA), σ_{LCA} .*

Process	$\sigma_{\text{LCA}} \pm \varepsilon$ (nb)	ε (%)	$\sigma_{\text{LCA}}/\sigma_{\text{EXACT}}$
$gg \rightarrow 2g$	$(0.46060 \pm 0.00308) \times 10^4$	0.7	1.0
$gg \rightarrow 3g$	$(0.15040 \pm 0.00159) \times 10^3$	1.0	1.0
$gg \rightarrow 4g$	$(0.12613 \pm 0.00187) \times 10^2$	1.5	1.1
$gg \rightarrow 5g$	$(0.09806 \pm 0.00196) \times 10^1$	2.0	1.0
$gg \rightarrow 6g$	$(0.69370 \pm 0.01736) \times 10^{-1}$	2.5	0.9
$gg \rightarrow u\bar{u}$	$(0.44170 \pm 0.00239) \times 10^2$	0.5	1.2
$gg \rightarrow g u\bar{u}$	$(0.40539 \pm 0.00456) \times 10^1$	1.1	1.1
$gg \rightarrow 2g u\bar{u}$	$(0.56107 \pm 0.01008) \times 10^0$	1.8	1.1
$gg \rightarrow 3g u\bar{u}$	$(0.60952 \pm 0.01771) \times 10^{-1}$	2.9	1.2
$gg \rightarrow 4g u\bar{u}$	$(0.56299 \pm 0.01552) \times 10^{-2}$	2.7	1.1
$gg \rightarrow c\bar{c}c\bar{c}$	$(0.31180 \pm 0.00612) \times 10^{-2}$	2.0	1.2
$gg \rightarrow g c\bar{c}c\bar{c}$	$(0.73387 \pm 0.02022) \times 10^{-3}$	2.7	1.2
$gg \rightarrow 2g c\bar{c}c\bar{c}$	$(0.11462 \pm 0.00377) \times 10^{-3}$	3.3	1.2

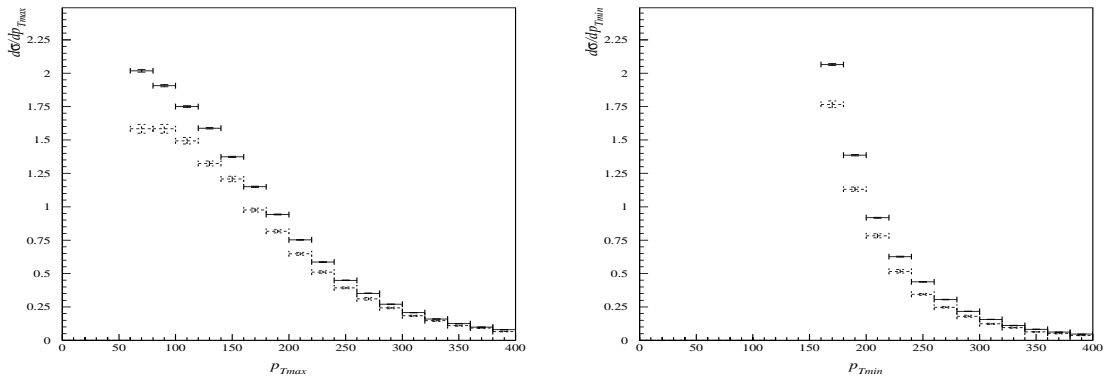


Figure 9: *Transverse momentum distribution of the most (left panel) and the less (right panel) energetic gluon in $gg \rightarrow 4g$ process. Solid line crosses denote SPHEL case whereas dashed, the Monte Carlo one.*

where $n \geq 4$ and smaller in case when $q\bar{q}$ pairs are present. In the Tab. 7. corresponding factors are presented. In principle the total cross sections can be corrected by setting the

Table 7: Results for the total cross section for specific helicity configuration approximation (SPHEL), σ_{SPHEL} .

Process	$\sigma_{\text{SPHEL}} \pm \varepsilon$ (nb)	ε (%)	$\sigma_{\text{SPHEL}}/\sigma_{\text{EXACT}}$
$gg \rightarrow 2g$	$(0.46508 \pm 0.00130) \times 10^4$	0.3	1.0
$gg \rightarrow 3g$	$(0.15187 \pm 0.00036) \times 10^3$	0.2	1.0
$gg \rightarrow 4g$	$(0.14108 \pm 0.00034) \times 10^2$	0.2	1.2
$gg \rightarrow 5g$	$(0.13105 \pm 0.00039) \times 10^1$	0.3	1.3
$gg \rightarrow 6g$	$(0.11530 \pm 0.00039) \times 10^0$	0.3	1.5
$gg \rightarrow u\bar{u}$	$(0.44789 \pm 0.00061) \times 10^2$	0.1	1.2
$gg \rightarrow g u\bar{u}$	$(0.40402 \pm 0.00101) \times 10^1$	0.2	1.1
$gg \rightarrow 2g u\bar{u}$	$(0.32118 \pm 0.00121) \times 10^0$	0.3	0.6
$gg \rightarrow 3g u\bar{u}$	$(0.25893 \pm 0.00138) \times 10^{-1}$	0.5	0.5
$gg \rightarrow 4g u\bar{u}$	$(0.20453 \pm 0.00125) \times 10^{-2}$	0.6	0.4
$gg \rightarrow c\bar{c}c\bar{c}$	$(0.27384 \pm 0.00084) \times 10^{-2}$	0.3	1.1
$gg \rightarrow g c\bar{c}c\bar{c}$	$(0.23113 \pm 0.00103) \times 10^{-3}$	0.4	0.4
$gg \rightarrow 2g c\bar{c}c\bar{c}$	$(0.17330 \pm 0.00144) \times 10^{-4}$	0.8	0.2

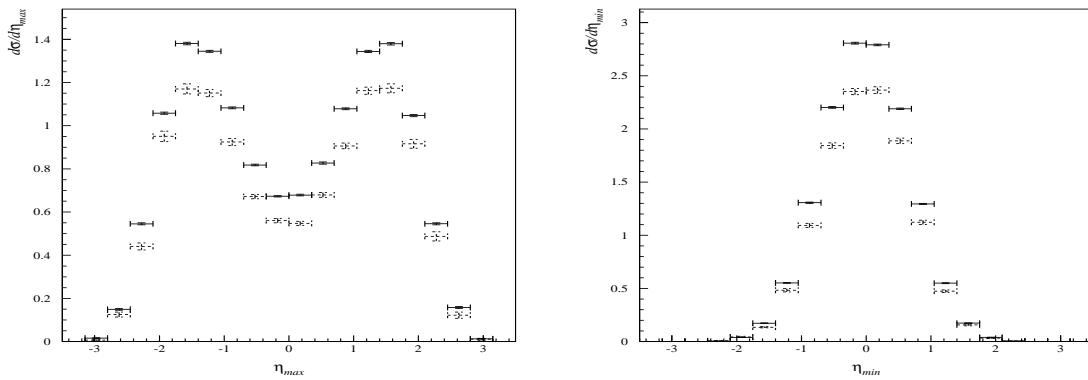


Figure 10: Rapidity distribution of the most (left panel) and the less (right panel) energetic gluon in $gg \rightarrow 4g$ process. Solid line crosses denote SPHEL case whereas dashed, the Monte Carlo one.

relevant weight factors for each process, however, they depend on the collider energy and on the phase space cuts. Instead SPHEL performs better in the shape of the distributions

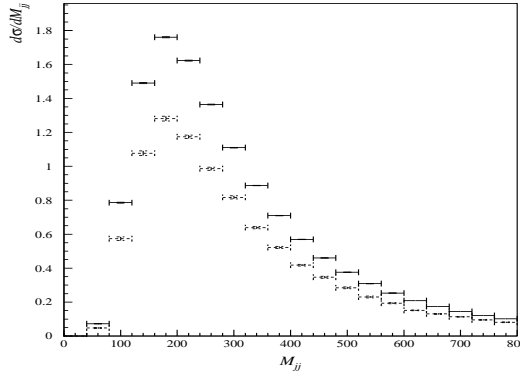


Figure 11: *Invariant mass distribution of 2 gluons in the $gg \rightarrow 5g$ process. Solid line crosses denote SPHEL case whereas dashed, the Monte Carlo one.*

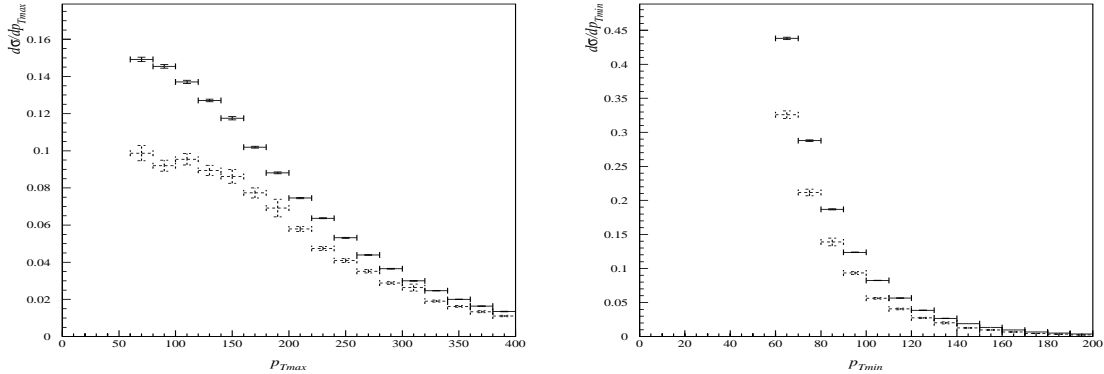


Figure 12: *Transverse momentum distribution of the most (left panel) and the less (right panel) energetic gluon in $gg \rightarrow 5g$ process. Solid line crosses denote SPHEL case whereas dashed, the Monte Carlo one.*

rather than in their normalisation. Corresponding distributions of invariant mass of 2-partons as well as rapidity and transverse momentum of the most and the less energetic parton for $gg \rightarrow 4g$ and $gg \rightarrow 5g$ processes are shown in Fig. 8.–Fig. 13.

In order to demonstrate that the Monte Carlo over colour does give the same information on the colour connection structure of the process, we examine in Fig. 14 the distribution of the following variable,

$$z = \frac{|\mathcal{M}_{\text{one}}|^2}{\sum_{i=1}^{\text{all}} |\mathcal{M}_i|^2} \quad (54)$$

where $|\mathcal{M}_{\text{one}}|^2$ is the square matrix element for one particular colour connection or colour flow configuration, normalised to the sum of all possible ones. In case of $g(1)g(2) \rightarrow g(3)g(4)$ process, the following colour flow $(1 \rightarrow 3 \rightarrow 4 \rightarrow 2 \rightarrow 1)$ has been plotted. This chain of numbers show how gluons are colour connected with each other. For the $g(1)g(2) \rightarrow g(3)g(4)g(5)$ process in the Fig. 14, the colour flow $(1 \rightarrow 5 \rightarrow 3 \rightarrow 2 \rightarrow 4 \rightarrow 1)$ is used.

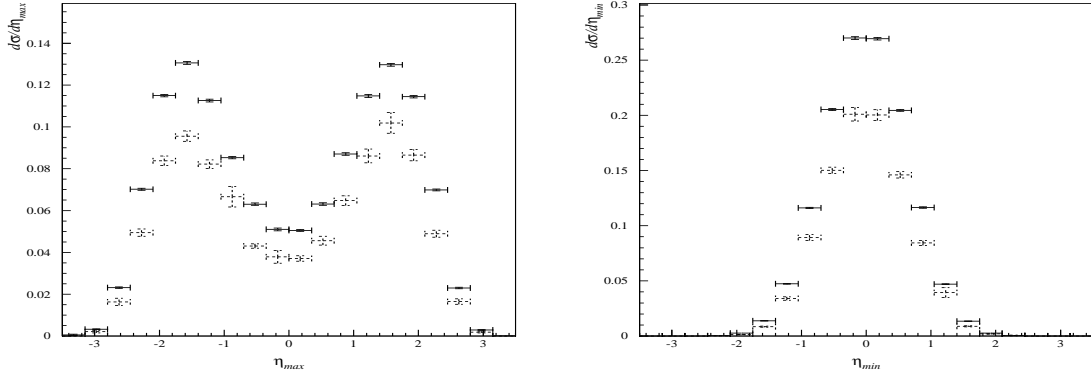


Figure 13: Rapidity distribution of the most (left panel) and the less (right panel) energetic gluon in $gg \rightarrow 5g$ process. Solid line crosses denote SPHEL case whereas dashed, the Monte Carlo one.

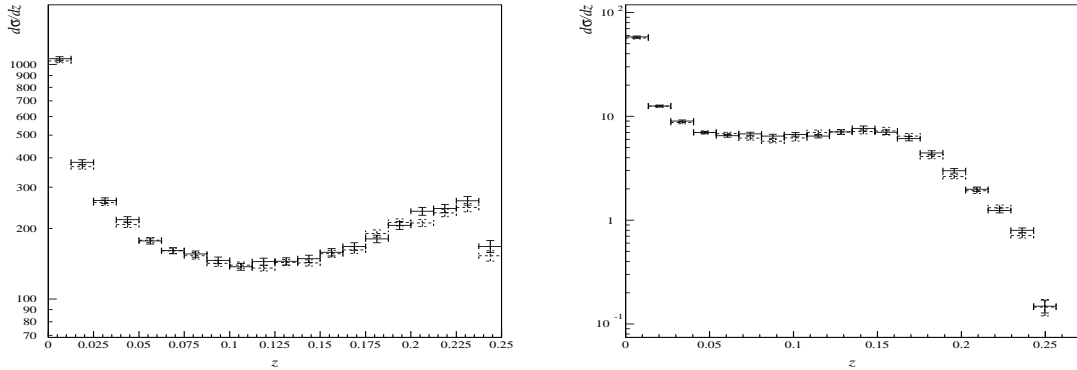


Figure 14: Distribution in $z = |\mathcal{M}_{\text{one}}|^2 / \sum_i^{\text{all}} |\mathcal{M}_i|^2$, where $|\mathcal{M}_{\text{one}}|^2$ is the square matrix element for one particular colour configuration normalised to the sum of all possible. The left-hand side plot corresponds to the $gg \rightarrow 2g$ process, the right-hand side one to the $gg \rightarrow 3g$. Solid line crosses denote summation over all colour configurations whereas dashed, the Monte Carlo summation.

The z variable distribution is what it could be used in order to pass colour connection information needed by a parton shower calculation. The agreement between the 'exact' and MC treatments proves that the latter one describes correctly the colour structure of the amplitude and that the merging of parton level calculation with the parton shower evolution can be safely performed in order to achieve a complete description of the fully hadronised final states observed in the real experiments.

Before closing this section, and in order to shed some light on the myth that, what is usually called 'analytical' expressions, result in a faster computation than the recursive equations implemented numerically, we present a comparison of the computational time for squared matrix element calculations between the analytical formulas as used by SPHEL and the recursive relations, used in this paper. In the Tab. 8 the computational time for SPHEL, MC as well as their ratio is presented in arbitrary units. As we can see for

Table 8: *Comparison of the computational time for squared matrix element calculation with the analytical formula of SPHEL and with the recursive approach. In the last columns their ratio is presented. Time values are given in some arbitrary units.*

Process	t_{SPHEL}	t_{MC}	$t_{\text{MC}}/t_{\text{SPHEL}}$
$gg \rightarrow 2g$	0.372×10^{-3}	0.519×10^{-1}	139.52
$gg \rightarrow 3g$	0.776×10^{-3}	0.135×10^0	173.97
$gg \rightarrow 4g$	0.252×10^{-2}	0.364×10^0	144.44
$gg \rightarrow 5g$	0.122×10^{-1}	0.143×10^1	117.21
$gg \rightarrow 6g$	0.806×10^{-1}	0.497×10^1	61.66
$gg \rightarrow 7g$	0.639×10^0	0.133×10^2	20.81
$gg \rightarrow 8g$	0.569×10^1	0.334×10^2	5.87
$gg \rightarrow 9g$	0.567×10^2	0.923×10^2	1.63
$gg \rightarrow 10g$	0.620×10^3	0.267×10^3	0.43

$n = 12$ the analytical formula is not faster any more then the recursive approach. In fact the SPHEL shows up a factorial growth in computational time, i.e. $n!$ whereas the recursive approach is just exponential, 3^n . For SPHEL this is because the number of possible momenta permutations is proportional to $n!$, as is easily seen in Eq.(17).

Summary and Outlook

In this work an efficient way for the computation of tree level amplitudes for multi-parton processes in the Standard Model was presented. The algorithm is based on the Dyson-Schwinger recursive equations. We discussed how the summation over colour configurations can be turned into a Monte Carlo summation, which proved to be more efficient, especially for a large number of coloured partons. Additionally, a set of typical results for total cross sections and differential distributions have been given. Moreover, a new algorithm for phase-space generation has been presented and used. The complete package can be used to generate, efficiently and reliably, any process with any number of external legs, for $n \leq 12$, in the Standard Model.

Our future interest includes a systematic study of fully hadronic final states in $p\bar{p}$ and pp collisions which requires the merging of the parton level calculations with parton shower and hadronization algorithms, *e.g* interfacing our package with codes like PYTHIA [35] or HERWIG [36]. The development of this kind of multipurpose Monte Carlo generators will certainly be of great interest in the study of TeVatron, LHC and e^+e^- Linear Collider data.

Acknowledgments

Work supported by the Polish State Committee for Scientific Research Grants number 1 P03B 009 27 for years 2004-2005 (M.W.). In addition, M.W. acknowledges the Maria Curie Fellowship granted by the European Community in the framework of the Human Potential Programme under contract HPMD-CT-2001-00105 (“*Multi-particle production and higher order correction*”). The Greece-Poland bilateral agreement “*Advanced computer techniques for theoretical calculations and development of simulation programs for high energy physics experiments*” is also acknowledged.

Appendix

In case of scattering of two hadrons it is useful to describe the final state in terms of transverse momentum p_T , azimuthal angle ϕ and rapidity y variables. These variables transform simply under longitudinal boosts which is useful in case of the parton-parton scattering where the centre of mass system is boosted with respect to that of the two incoming hadrons. In terms of p_T , ϕ and y the four-momentum of a massless particle can be written as

$$p^\mu = (E, p^x, p^y, p^z) = (p_T \cosh y, p_T \cos \phi, p_T \sin \phi, p_T \sinh y) \quad (55)$$

It is much more natural to express the phase space volume for a system of n particles

$$V_n = \int \delta^4(P - \sum_{i=1}^n p_i) \prod_{i=1}^n d^4 p_i \delta(p_i^2 - m_i^2) \Theta(p_i^0) \quad (56)$$

using p_T , ϕ and y variables

$$V_n = \int \delta^4(P - \sum_{i=1}^n p_i) \prod_{i=1}^n p_{T_i} dp_{T_i} dy_i d\phi_i. \quad (57)$$

To derive the above expression, which lead us to the Monte Carlo algorithm, we follow method presented in Ref. [32]. We start by defining the phase-space-like object

$$V_0 = \int_0^\infty \left(\prod_{i=2}^n dk_{T_i} P(k_{T_i}) \right) \int_0^{2\pi} \left(\prod_{i=2}^n d\phi_i \right) \int_{-\infty}^{+\infty} \left(\prod_{i=2}^n d\bar{y}_i \Pi(\bar{y}_i) \right) \quad (58)$$

describing a system of n four momenta that are not constrained by momentum conservation but occur with some weight functions $P(k_{T_i})$, $\Pi(\bar{y}_i)$ which keeps the total volume finite. In the next step we have to relate the new variables to the physical ones p_{T_i} , y_i and ϕ_i :

$$\begin{aligned} V_0 = & \int_0^\infty \left(\prod_{i=2}^n dk_{T_i} P(k_{T_i}) \right) \int_0^{2\pi} \left(\prod_{i=2}^n d\phi_i \right) \int_{-\infty}^{+\infty} \left(\prod_{i=2}^n d\bar{y}_i \Pi(\bar{y}_i) \right) \\ & \int_0^\infty \left(\prod_{i=1}^n dp_{T_i} \delta(p_{T_i} - xk_{T_i}) \right) \int_{-\infty}^{+\infty} \left(\prod_{i=2}^n dy_i \delta(\bar{y}_i + y_{i-1} - y_i) \right) \\ & \int_0^\infty dk_{T_1} \int_0^{2\pi} d\phi_1 \delta(x \sum_{i=2}^n k_{T_i} \cos \phi_i) \delta(x \sum_{i=2}^n k_{T_i} \sin \phi_i) \mathcal{J}_1 \end{aligned} \quad (59)$$

$$\int_0^\infty dx \int_{-\infty}^{+\infty} dy_1 \delta(x \sum_{i=2}^n k_{T_i} \cosh y_i - E) \delta(x \sum_{i=2}^n k_{T_i} \sinh y_i - L) \mathcal{J}_2.$$

with the Jacobians \mathcal{J}_1 and \mathcal{J}_2 :

$$\mathcal{J}_1 = \left| \frac{\partial(x \sum k_{T_i} \cos \phi_i, x \sum k_{T_i} \sin \phi_i)}{\partial(k_{T_1}, \phi_1)} \right| = x^2 k_{T_1} \quad (60)$$

$$\mathcal{J}_2 = \left| \frac{\partial(x \sum k_{T_i} \cosh y_i - E, x \sum k_{T_i} \sinh y_i - L)}{\partial(x, y_1)} \right| = \frac{E^2 - L^2}{x}. \quad (61)$$

E and L represents energy and longitudinal part of the initial two particles. We proceed with integration where the different arguments of the various δ functions were manipulated in order to perform the integral

$$\int_0^\infty \prod_{i=1}^n dk_{T_i} \delta(p_{T_i} - xk_{T_i}) \quad (62)$$

$$\int_{-\infty}^{+\infty} \prod_{i=2}^n d\bar{y}_i \delta(\bar{y}_i + y_{i-1} - y_i). \quad (63)$$

We are left with

$$V_0 = \int \delta^4(P - \sum_{i=1}^n p_i) \left(\prod_{i=1}^n p_{T_i} dp_{T_i} dy_i d\phi_i \right) \left(\prod_{i=2}^n P\left(\frac{p_{T_i}}{x}\right) \frac{1}{p_{T_i}} \Pi(\bar{y}_i) \right) (E^2 - L^2) \frac{2^n}{x^n} dx. \quad (64)$$

We are free of choosing the distribution functions so that the total volume is kept finite. The criterion used is to minimize the variance, by taking into account the anticipated form of the multi-parton matrix elements, so we introduce

$$P(x) = \frac{1}{a} \exp\left(\frac{-x}{a}\right), \quad \Pi(\bar{y}) = \frac{\tanh(2\eta + \bar{y}) + \tanh(2\eta - \bar{y})}{8\eta} \quad (65)$$

where $a > 0$ and perform the integration over dx

$$\int_0^\infty \left(\prod_{i=2}^n \frac{1}{a} \exp\left(\frac{-p_{T_i}}{xa}\right) \frac{1}{p_{T_i}} \right) \frac{1}{x^n} dx = \left(\prod_{i=2}^n \frac{1}{p_{T_i}} \right) \left(\sum_{i=2}^n p_{T_i} \right)^{-n+1} \Gamma(n-1). \quad (66)$$

We finally arrive at the formula

$$V_0 = \int \delta^4(P - \sum_{i=1}^n p_i) \left(\prod_{i=1}^n p_{T_i} dp_{T_i} dy_i d\phi_i \right) \times \quad (67)$$

$$\left(\prod_{i=2}^n \frac{1}{p_{T_i}} \right) \left(\sum_{i=2}^n p_{T_i} \right)^{-n+1} \Gamma(n-1) \left(\prod_{i=2}^n \Pi(\bar{y}_i) \right) (E^2 - L^2) 2^n.$$

On the other hand if we applied Eq.(65) to the formula Eq.(58) we can find

$$\int_0^\infty \left(\prod_{i=2}^n dk_{T_i} \frac{1}{a} \exp\left(\frac{-k_{T_i}}{a}\right) \right) = 1 \quad (68)$$

$$\int_{-\infty}^{+\infty} \left(\prod_{i=2}^n d\bar{y}_i \Pi(\bar{y}_i) \right) = (8\eta)^{n-1} \quad (69)$$

$$\int_0^{2\pi} \left(\prod_{i=3}^n d\phi_i \right) = (2\pi)^{n-1} \quad (70)$$

and

$$V_0 = (2\pi \cdot 8\eta)^{n-1}. \quad (71)$$

The weight of the event is given by

$$W = \frac{(2\pi \cdot 8\eta)^{n-1}}{S_n} \quad (72)$$

where

$$S_n = \int dp_{T_i} dy_i d\phi_i \left(\prod_{i=2}^n \frac{1}{p_{T_i}} \right) \left(\sum_{i=2}^n p_{T_i} \right)^{-n+1} \Gamma(n-1) \left(\prod_{i=2}^n \Pi(\bar{y}_i) \right) (E^2 - L^2) 2^n.$$

In the next step we translate this description into Monte Carlo procedure and generate independently n variables k_{T_i} , ϕ_i and $\bar{y}_i = y_i - y_{i-1}$ and assuming that $\phi_1 = 0$ as well as $y_1 = 0$. Using the symbol ρ_i to denote a random number uniformly distributed in $(0, 1)$ we do this as follows:

$$k_{T_i} = -a \log \rho_i, \quad i = 2, \dots, n \quad (73)$$

$$\phi_i = 2\pi \rho_i, \quad i = 2, \dots, n \quad (74)$$

where a is a free parameter. For \bar{y}_i variable we proceed in few steps starting with

$$F_i = \exp(4\eta(2\rho_i - 1)) \quad i = 2, \dots, n \quad (75)$$

where η is a free parameter and

$$\cosh \bar{y}_i = \frac{(F_i + 1) \sinh 2\eta}{\mathcal{Z}_i}, \quad \sinh \bar{y}_i = \frac{(F_i - 1) \cosh 2\eta}{\mathcal{Z}_i} \quad (76)$$

where

$$\mathcal{Z}_i = \sqrt{2F_i \cosh 4\eta - (1 + F_i^2)}. \quad (77)$$

To complete the description of the algorithm we have to find expression for k_{T_1} , ϕ_1 and y_1 variables. We start by defining the transversal part of the $2, \dots, n$ system as follows

$$X \equiv \sum_{i=2}^n k_{T_i} \cos \phi_i, \quad Y \equiv \sum_{i=2}^n k_{T_i} \sin \phi_i. \quad (78)$$

From these equations we have the following relations for k_{T_1} and ϕ_1 to be able to describe the total n particle system

$$\cos \phi_1 = -\frac{X}{k_{T_1}}, \quad \sin \phi_1 = -\frac{Y}{k_{T_1}} \quad (79)$$

where

$$k_{T_1} = \sqrt{X^2 + Y^2}. \quad (80)$$

The total energy and total longitudinal part of the system are represented by

$$\mathcal{E} = k_{T_1} + k_{T_2} \cosh(\bar{y}_2) + k_{T_3} \cosh(\bar{y}_3 + \bar{y}_2) + \dots \quad (81)$$

$$\mathcal{L} = k_{T_2} \sinh(\bar{y}_2) + k_{T_3} \sinh(\bar{y}_3 + \bar{y}_2) + \dots \quad (82)$$

so y_1 is given by

$$\cosh y_1 = \frac{\mathcal{E}E - \mathcal{L}L}{\sqrt{\mathcal{E}^2 - \mathcal{L}^2}\sqrt{E^2 - L^2}}, \quad (83)$$

$$\sinh y_1 = \frac{-\mathcal{L}E + \mathcal{E}L}{\sqrt{\mathcal{E}^2 - \mathcal{L}^2}\sqrt{E^2 - L^2}}, \quad (84)$$

$$x = \sqrt{\frac{E^2 - L^2}{\mathcal{E}^2 - \mathcal{L}^2}}. \quad (85)$$

Finally to get the final four momenta p_i^μ the following transformations are used:

$$E_i = xk_{T_i} \cosh y_i \quad (86)$$

$$p_i^x = xk_{T_i} \cos \phi_i \quad (87)$$

$$p_i^y = xk_{T_i} \sin \phi_i \quad (88)$$

$$p_i^z = xk_{T_i} \sinh y_i. \quad (89)$$

This completes the description of the algorithm we have to supplemented it with the prescription for the weight of a generated event which is given by Eq.(72).

References

- [1] M. A. Dobbs *et al.*, “Les Houches Guidebook to Monte Carlo Generators for Hadron Collider Physics”, [hep-ph/0403045](#).
- [2] F. Maltoni and T. Stelzer, “Madevent: Automatic event generation with MadGraph”, *JHEP* **02** (2003) 027, [hep-ph/0208156](#).
- [3] F. Krauss, R. Kuhn, and G. Soff, “Amegic++ 1.0: A matrix element generator in C++”, *JHEP* **02** (2002) 044, [hep-ph/0109036](#).
- [4] M. L. Mangano, M. Moretti, F. Piccinini, R. Pittau, and A. D. Polosa, “ALPGEN, a generator for hard multiparton processes in hadronic collisions”, *JHEP* **07** (2003) 001, [hep-ph/0206293](#).
- [5] M. L. Mangano and S. J. Parke, “Multiparton amplitudes in gauge theories”, *Phys. Rept.* **200** (1991) 301.
- [6] F. A. Berends, R. Kleiss, P. De Causmaecker, R. Gastmans, and T. T. Wu, “Single bremsstrahlung processes in gauge theories”, *Phys. Lett.* **B103** (1981) 124.
- [7] S. J. Parke and T. R. Taylor, “Perturbative QCD utilizing extended supersymmetry”, *Phys. Lett.* **B157** (1985) 81.
- [8] S. J. Parke and T. R. Taylor, “Gluonic two goes to four”, *Nucl. Phys.* **B269** (1986) 410.
- [9] Z. Kunszt, “Combined use of the calkul method and N=1 supersymmetry to calculate QCD six parton processes”, *Nucl. Phys.* **B271** (1986) 333.

- [10] F. A. Berends and W. Giele, “The six gluon process as an example of Weyl-Van der Waerden spinor calculus”, *Nucl. Phys.* **B294** (1987) 700.
- [11] M. L. Mangano, S. J. Parke, and Z. Xu, “Duality and multi - gluon scattering”, *Nucl. Phys.* **B298** (1988) 653.
- [12] S. J. Parke and T. R. Taylor, “An amplitude for n gluon scattering”, *Phys. Rev. Lett.* **56** (1986) 2459.
- [13] F. A. Berends and W. T. Giele, “Recursive calculations for processes with n gluons”, *Nucl. Phys.* **B306** (1988) 759.
- [14] R. Kleiss and W. J. Stirling, “Spinor techniques for calculating $p\bar{p} \rightarrow W^\pm/Z^0 + \text{jets}$ ”, *Nucl. Phys.* **B262** (1985) 235.
- [15] J. F. Gunion and Z. Kunszt, “Improved analytic techniques for tree graph calculations and the $gg q\bar{q}$ lepton antilepton subprocess”, *Phys. Lett.* **B161** (1985) 333.
- [16] Z. Xu, D.-H. Zhang, and L. Chang, “Helicity amplitudes for multiple bremsstrahlung in massless nonabelian gauge theories”, *Nucl. Phys.* **B291** (1987) 392.
- [17] J. G. M. Kuijf, “Multiparton production at hadron colliders”, Ph.D.Thesis, University of Leiden 1991, RX-1335.
- [18] W. T. Giele, “Properties and calculations of multiparton processes”, Ph.D.Thesis, University of Leiden 1989, RX-1267.
- [19] F. Caravaglios and M. Moretti, “An algorithm to compute born scattering amplitudes without Feynman graphs”, *Phys. Lett.* **B358** (1995) 332–338, [hep-ph/9507237](#).
- [20] F. Caravaglios, M. L. Mangano, M. Moretti, and R. Pittau, “A new approach to multi-jet calculations in hadron collisions”, *Nucl. Phys.* **B539** (1999) 215, [hep-ph/9807570](#).
- [21] P. Draggiotis, R. H. P. Kleiss, and C. G. Papadopoulos, “On the computation of multigluon amplitudes”, *Phys. Lett.* **B439** (1998) 157, [hep-ph/9807207](#).
- [22] A. Kanaki and C. G. Papadopoulos, “Helac: A package to compute electroweak helicity amplitudes”, *Comput. Phys. Commun.* **132** (2000) 306, [hep-ph/0002082](#).
- [23] A. Kanaki and C. G. Papadopoulos, “Helac-phegas: Automatic computation of helicity amplitudes and cross sections”, Published in AIP Conference Proceedings – August 20, 2001 – Volume 583, Issue 1, pp. 169-172 and in Workshop On Computer Particle Physics: (CPP 2001): Automatic Calculation For Future Colliders, edited by Y. Kurihara. Tsukuba, Japan, KEK, 2002. 189p. (KEK-PROCEEDINGS-2002-11), p. 20-25, [hep-ph/0012004](#).
- [24] P. D. Draggiotis, R. H. P. Kleiss, and C. G. Papadopoulos, “Multi-jet production in hadron collisions”, *Eur. Phys. J.* **C24** (2002) 447, [hep-ph/0202201](#).
- [25] F. Maltoni, K. Paul, T. Stelzer, and S. Willenbrock, “Color-flow decomposition of QCD amplitudes”, *Phys. Rev.* **D67** (2003) 014026, [hep-ph/0209271](#).

- [26] P. D. Draggiotis, “Exploding QCD - enumeration and computation of QCD processes”, PhD Thesis, University of Nijmegen 2002.
- [27] J. Pumplin *et al.*, “New generation of parton distributions with uncertainties from global QCD analysis”, *JHEP* **07** (2002) 012, [hep-ph/0201195](#).
- [28] D. Stump *et al.*, “Inclusive jet production, parton distributions, and the search for new physics”, *JHEP* **10** (2003) 046, [hep-ph/0303013](#).
- [29] C. G. Papadopoulos, “Phegas: A phase space generator for automatic cross-section computation”, *Comput. Phys. Commun.* **137** (2001) 247, [hep-ph/0007335](#).
- [30] R. Kleiss and R. Pittau, “Weight optimization in multichannel Monte Carlo”, *Comput. Phys. Commun.* **83** (1994) 141, [hep-ph/9405257](#).
- [31] A. van Hameren and C. G. Papadopoulos, “A hierarchical phase space generator for QCD antenna structures”, *Eur. Phys. J.* **C25** (2002) 563, [hep-ph/0204055](#).
- [32] R. Kleiss, W. J. Stirling, and S. D. Ellis, “A new Monte Carlo treatment of multi-particle phase space at high-energies”, *Comput. Phys. Commun.* **40** (1986) 359.
- [33] C. G. Papadopoulos and M. Worek, “Multi-particle processes in QCD without Feynman diagrams”, [hep-ph/0508291](#).
- [34] C. G. Papadopoulos and M. Worek, “Multi-particle processes in the Standard Model without Feynman diagrams”, *Acta Phys. Polon.* **B36** (2005) 3355, [hep-ph/0510416](#).
- [35] T. Sjostrand *et al.*, “High-energy-physics event generation with PYTHIA 6.1”, *Comput. Phys. Commun.* **135** (2001) 238, [hep-ph/0010017](#).
- [36] G. Corcella *et al.*, “HERWIG 6: An event generator for hadron emission reactions with interfering gluons (including supersymmetric processes)”, *JHEP* **01** (2001) 010, [hep-ph/0011363](#).